



Removal of NO_x and soot over Ce/Zr/K/Me (Me = Fe, Pt, Ru, Au) oxide catalysts



Roberto Matarrese ^a, Sara Morandi ^b, Lidia Castoldi ^a, Pierluigi Villa ^c, Luca Lietti ^{a,*}

^a Dipartimento di Energia, Laboratory of Catalysis and Catalytic Processes and NEMAS, Centre of Excellence, Politecnico di Milano, P.zza L. da Vinci 32, 20156 Milano, Italy

^b Dipartimento di Chimica and NIS, Center of Excellence, Università di Torino, Via P. Giuria 7, 10125, Torino, Italy

^c Dipartimento di Chimica Ingegneria Chimica e Materiali, Università degli Studi dell'Aquila, Via Gronchi 18, Zona industriale di Pile, 67100 L'Aquila, Italy

ARTICLE INFO

Article history:

Received 25 April 2016

Received in revised form 1 July 2016

Accepted 14 July 2016

Available online 2 August 2016

Keywords:

Soot oxidation

Combined soot and NO_x removal

Ceria/Zirconia

Ruthenium

FT-IR spectroscopy

ABSTRACT

The potentiality of ceria/zirconia based catalysts in the simultaneous removal of particulate matter (soot) and NO_x is investigated in this work, and compared with that of a model LNT Pt-K/Al₂O₃ sample. Ceria-zirconia (molar ratio 75/25) catalysts doped with Pt, Au, Ru or Fe (2% by weight) and containing K (7% by weight) were prepared by a modified citrate method and characterized by X-ray diffraction, surface area and pore volume measurements. The behavior of the catalysts in the soot combustion and NO_x removal was separately analyzed by means of temperature programmed oxidation (TPO), isothermal combustion and isothermal NO_x adsorption experiments. The results showed that all the ceria/zirconia based catalysts are more active than Pt-K/Al₂O₃ in soot combustion; the Ru-containing system also showed NO_x storage performances comparable to Pt-K/Al₂O₃. Accordingly the capability of the Ru-based catalyst to accomplish the removal of NO_x in the absence and in the presence of soot was further investigated by reactivity experiments and FT-IR spectroscopy to analyze both the gas phase and the catalyst surface species. The data indicate that the Ru-based system is able to simultaneously remove soot and adsorb NO_x pointing out higher performances in the soot combustion as compared to the Pt-K/Al₂O₃ catalyst, and similar behavior in the NO_x storage capacity. However the NO_x reduction activity results lower than the traditional LNT Pt-based catalyst. Conversely, when the Ru-based catalyst is mixed with the LNT sample (physical mixture) a NO_x reduction efficiency similar to Pt-K/Al₂O₃ is found.

© 2016 Elsevier B.V. All rights reserved.

1. Introduction

The main pollutants emitted by diesel engines are nitrogen oxides and particulate matter (i.e. soot) whose hazardous effects on both environment and public health are widely recognized. For this reason, during the last decades the development and application of catalytic technologies for the control of polluting emissions from diesel vehicles have grown dramatically, forced by the application of stringent legislative emissions standards such as Euro 6 or U.S. Tier 2.

Among the deNO_x after treatment technologies, selective catalytic reduction (SCR) of NO_x with ammonia/urea [1] and NO_x storage reduction (NSR) technique, also quoted as lean NO_x trap (LNT) [2,3], represent the most viable solutions. On the other hand, the control of soot emissions is currently accomplished by the use of

the so-called diesel particulate filters (DPFs) [4] on which soot contained in the exhausts is accumulated. For this reason, DPFs need to be periodically regenerated in order to avoid pressure drops, which potentially decrease the engine efficiency. Regeneration is usually performed by increasing the filter temperature (active regeneration) so that the particulate is burnt by oxygen present in the exhausts. This process requires an extra fuel consumption, thus increasing fuel penalty; moreover, excessive heating can damage filter itself and the other catalytic aftertreatment devices (e.g. SCR and LNT units). It is therefore mandatory to reduce the temperature at which soot combustion is attained.

A possible solution consists in the coating of the DPF with an oxidation catalyst [5] in order to promote soot combustion at temperatures near the engine operating conditions (passive regeneration). However, one of the most critical aspects of catalytic filters is represented by the poor reactivity at low temperature; besides, they are not able to remove NO_x.

On this regard an integrated deNO_x-deSoot after-treatment technique, known as DPNR (Diesel Particulate- NO_x Reduction), has

* Corresponding author.

E-mail address: luca.lietti@polimi.it (L. Lietti).

been developed by Toyota [6]. This system consists of both a new catalytic filter and a new diesel combustion technology which has the unique capacity to remove simultaneously both soot and NO_x . The new catalytic converter for DPNR is a porous ceramic wall-flow filter coated with a LNT catalytic layer constituted by a high surface area support (e.g. γ -alumina), by a noble metal (e.g. Pt and/or Rh) and by an alkaline or alkaline-earth metal oxide which presents a high NO_x -storage capacity. Like LNTs, DPNR systems work under cyclic conditions, alternating long lean phases with short regeneration phases under rich condition: during the lean phase the NO_x produced by the engine are oxidized and subsequently adsorbed on the alkaline or alkaline-earth metal oxide component, while during the rich phase the NO_x stored species are then reduced to molecular nitrogen by CO , H_2 and unburnt hydrocarbons. The particulate matter removal takes place mainly under lean conditions by oxygen and NO_2 formed upon NO oxidation over noble metals even if Toyota researchers proposed that active oxygen species, which are formed during NO_x adsorption, can promote soot oxidation also under rich conditions as well.

In previous works of our group we have investigated the reactivity of model $\text{Pt-Ba/Al}_2\text{O}_3$ and $\text{Pt-K/Al}_2\text{O}_3$ DPNR catalysts in both the NO_x storage/reduction and soot oxidation. It was found that these systems are able to store NO_x under lean conditions even in the presence of soot while soot combustion is simultaneously occurring [7–10]. The effect of soot on the NO_x storage and reduction activity was also analyzed [10–14] pointing out that the presence of soot does not appreciably affect the reduction of the stored NO_x , while inhibits the NO_x storage capacity. This was ascribed to the competition between soot and Ba/K sites for the reaction with NO_2 , i.e. soot offers another pathway for the utilization of NO_2 rather than the NO_x storage process. Besides a complex interplay between soot and the stored NO_x was pointed out, suggesting the direct participation of the surface NO_x species in the soot oxidation [15]. $\text{Pt-K/Al}_2\text{O}_3$ system showed higher performances in the soot oxidation if compared to Ba-based catalyst [8–10] likely due to the formation of mobile potassium surface compounds which favor the soot-catalyst contact and hence the reactivity.

To date, ceria-based oxides are considered among the most promising materials for soot combustion [16–24]. This is ascribed to the ability of ceria to change oxidation state (i.e. by $\text{Ce}^{4+}/\text{Ce}^{3+}$ redox cycle) under oxygen rich operation conditions which allows facile oxygen uptake/release thus promoting the oxygen delivery from the lattice to the gas phase and hence to soot surface. Moreover ceria-based materials are able to accelerate the oxidation of NO to NO_2 , which is a stronger soot oxidant than oxygen [25], involving oxygen from the catalyst so promoting the soot oxidation. Moreover, the doping of ceria with proper cations, such as zirconium, can further increase surface oxygen availability and thus soot combustion.

On this basis, the aim of this work is to investigate the potentiality of novel LNT ceria-zirconia catalysts doped with Pt, Au, Ru or Fe and containing K as NO_x storage component for the simultaneous removal of NO_x and soot. In particular we have initially analyzed the behavior of all the catalysts in both the soot combustion and in the NO_x storage by means of temperature programmed oxidation (TPO) experiments and isothermal NO_x adsorption experiments. The reactivity of the most promising system (i.e. the Ru-containing ceria/zirconia sample) was further investigated in both the soot combustion and in the simultaneous removal of soot and NO_x .

For this purpose, microreactor studies and FT-IR analyses were used as complementary techniques to gain further information on both NO_x storage and reduction pathways. The behavior of a model $\text{Pt-K/Al}_2\text{O}_3$ LNT catalyst and that of combined catalyst configurations (i.e. a double-bed configuration with the LNT catalyst layer placed upstream the Ru-containing catalyst and a physical mixture

of the two catalyst samples in one layer) was also considered for comparison purposes.

2. Experimental

2.1. Catalysts preparation and characterization

K- and K/Me-doped (Me = Fe, Pt, Au, Ru) ceria-zirconia mixed oxides with a Ce/Zr molar ratio 75/25 were prepared by a modified citrate method [26,27]. A CeZr sample doped with 7% by weight of potassium (hereafter denoted as CZK) and a series of CZKMe (Me = Fe, Pt, Au, Ru) catalysts doped with 7% by weight of potassium and 2% by weight of Me (hereafter denoted as CZKFe, CZKPt, CZKAu and CZKRu, respectively) were prepared.

Briefly, the various precursors (cerium(III) acetate hydrate from Chempur, zirconium(IV) propoxide from Aldrich, potassium acetate from Carlo Erba, Iron(III) citrate from Aldrich, tetraammine platinum hydroxide from Heraeus, gold(III) hydroxide from Aldrich and ruthenium acetate from Chempur) were separately dissolved in an aqueous solution of citric acid monohydrate (Carlo Erba). All the solutions were then mixed and neutralized with ammonium hydroxide (Aldrich, 33% NH_3). The resulting solution was concentrated in rotavapor (Laborota 20 Control of Heidolph) and further dried under vacuum conditions at 230 °C for 10 h to obtain expanded meringue-like solids. The meringue thus obtained was crushed and sieved to obtain a powder. The decomposition of the organic part (i.e. citric acid) was performed in a fluidized bed system [28] at 330 °C operating with a nitrogen/air flow. A final calcination in air at 800 °C and then 900 °C for further 10 h was performed.

The obtained catalysts were characterized by X-ray powder diffraction (XRD) with a Bruker D8 instrument using graphite monochromated $\text{CuK}\alpha$ radiation; the diffraction patterns were collected in the 2 θ range of 10–90° with a step of 0.05° and a counting time of 12.5 s per step. BET Surface area and pore size distribution were measured by single point N_2 adsorption–desorption at –196 °C (Micromeritics TriStar 3000 Instrument).

For comparison purpose, an homemade $\text{Pt-K/Al}_2\text{O}_3$ (1/5.4/100 w/w) catalyst was also used. It was prepared by incipient wetness impregnation of a commercial alumina sample (Versal 250 from UOP) with aqueous solution of dinitro-diammine platinum (Strem Chemicals, 5% w/w Pt in ammonium hydroxide) and subsequently with a solution of potassium acetate (Aldrich). The powder was dried at 80 °C and calcined in air at 500 °C for 5 h after each impregnation step. A detailed characterization of the model $\text{Pt-K/Al}_2\text{O}_3$ catalyst is reported in previous works [10,29,30]. The specific surface area and pore volume are 167 m^2/g and 0.9 cm^3/g , respectively. The Pt dispersion, as determined by H_2 chemisorption at 0 °C, is about 30%. XRD patterns of the calcined sample show the characteristic peaks of microcrystalline γ - Al_2O_3 ; traces of monoclinic K_2CO_3 (JCPDS 16-820) and cubic K_2O (JCPDS 23-493) phases were also recognized.

Printex U (Evonik-Degussa) was used as model soot, which is widely used as a model substance for diesel particulate and whose properties are well described in the literature [31,32].

2.2. Catalytic tests

All reactivity tests were performed in a micro flow-reactor apparatus consisting of a quartz tube reactor (7 mm i.d.) connected to a mass spectrometer (Omnistar 200, Pfeiffer Vacuum), a micro-GC (Agilent 3000A) and an UV analyzer (Limas 11HW, ABB) for the on-line analysis of the outlet gases (NO, NO_2 , N_2 , H_2 , O_2 , CO, CO_2 , N_2O and NH_3). 59.4 mg of catalyst or 66 mg of the soot-catalyst mixture (corresponding to 59.4 mg of catalyst and 6.6 mg of soot) were used in each run. Catalyst-soot mixtures were prepared by gently mixing

in a vial the catalyst powder with soot (9:1 by weight catalyst/soot ratio), thus realizing a loose contact. The total gas flow was always set at 100 cm³/min (at 0 °C and 1 atm).

Catalytic tests were also performed using a physical mixture of the two Pt-K/Al₂O₃ + CZKRu samples (obtained by gently mixing the catalysts) and a double-bed configuration as well where the CZKRu catalyst is placed downstream the Pt-K/Al₂O₃ sample, separated by a quartz layer. In these cases 29.7 mg of each sample were used (total catalyst loading of 59.4 mg), while the total gas flow was always set at 100 cm³/min (at 0 °C and 1 atm) to maintain the same contact time of the individual samples.

The behavior of the catalysts in the soot combustion was addressed by means of temperature programmed oxidation (TPO) experiments and under isothermal conditions as well. In the case of TPO experiments, the soot–catalyst mixture is heated from room temperature to 750 °C (heating rate 10 °C/min) with O₂ (3% v/v, corresponding to 30 mbar) in He or O₂ (3% v/v) + NO (1000 ppm, corresponding to 1 mbar) + H₂O (1% v/v, corresponding to 10 mbar) + CO₂ (0.1% v/v, corresponding to 1 mbar) in He. In the case of isothermal reaction, the catalyst sample is heated at 350 °C in the same atmosphere for 4 h. Then a TPO experiment (up to 750 °C) was carried out to quantify the residual amount of soot.

The NO_x adsorption performances were investigated at 350 °C by admitting to the reactor a rectangular step feed of NO (1000 ppm) + 3% O₂ (v/v) in He and in the presence of H₂O (1% v/v) and CO₂ (0.1% v/v).

Finally, the NO_x storage and reduction activity was studied in the absence and in the presence of soot by performing lean-rich cycles at 300 °C (isothermal concentration step change experiments, ICSC). For this purpose, rectangular step feeds of NO (1000 ppm) + 3% O₂ (v/v) in He and of hydrogen (4000 ppm, corresponding to 40 mbar) in He, separated by a He purge in between, were alternatively fed to the reactor in the presence of H₂O (1% v/v) and CO₂ (0.1% v/v).

2.3. In situ FTIR study

Absorption/transmission IR spectra were run on a Perkin-Elmer FTIR System 2000 spectrophotometer equipped with a Hg–Cd–Te cryo-detector, working in the range of wavenumbers 7200–580 cm^{−1} at a resolution of 2 cm^{−1}. For IR analysis powder samples were compressed in self-supporting discs (10 mg cm^{−2}) and placed in a commercial heated stainless steel cell (Aabspec) allowing thermal treatments in situ under vacuum or controlled atmosphere and the simultaneous registration of spectra at temperatures up to 600 °C. The cell was equipped with single-crystal KBr windows. Experiments were carried out both on the single catalysts (Pt-K/Al₂O₃ and CZKRu) and on the physical mixture (1/1 w/w).

Before the measurements, the samples were treated at 600 °C in vacuum and dry oxygen in order to clean the surface from adsorbed species. After this activation stage, the samples were cooled down to the desired temperature (i.e. 250 and 300 °C) in oxygen and outgassed before the admission of the chosen atmosphere: NO (5 mbar), NO/O₂ 1:4 mixture (p_{NO} = 5 mbar) or H₂ (5 mbar). The results obtained at 250 °C are very similar to those obtained at 300 °C. However, at 300 °C the formation of broad electronic absorptions related to the semi-conducting properties of ceria, i.e. the ability of losing oxygen with the formation of lattice defects, makes the spectra noisy. For this reason, the spectra reported in the figures are those run at 250 °C. The spectra recorded during the interaction with a gas are reported as difference spectra in the figures: the spectrum subtracted is always that recorded after the activation treatment. In this way the bands related to surface species formed upon gas interactions are clearly visible.

Table 1

Morphological properties of the ceria/zirconia catalysts: surface area, pore volume and average pore diameter.

Catalytic systems	A _s [m ² /g]	V _p [cm ³ /g]	d _p [nm]
CZK	7.25	0.035	19.3
CZKRu	9.02	0.032	14.2
CZKPt	8.45	0.034	16.2
CZKAu	3.53	0.012	13.5
CZKFe	3.35	0.016	19.6

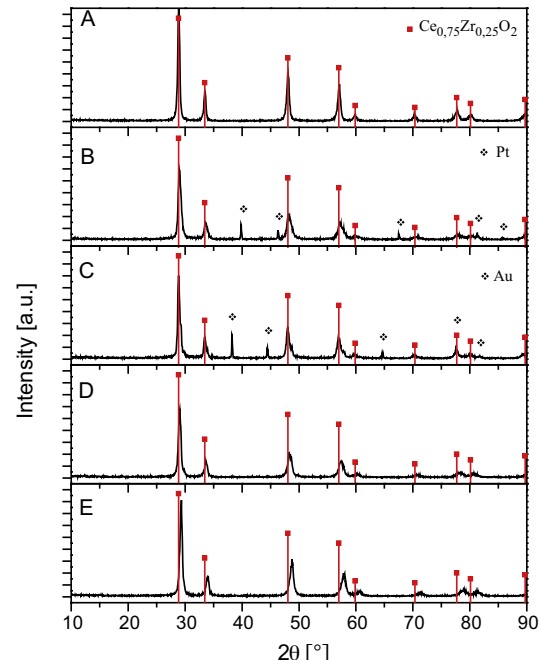


Fig. 1. XRD patterns of CZK (A), CZKPt (B), CZKAu (C), CZKFe (D) and CZKRu (E).

3. Results and discussion

3.1. Catalysts characterization

The surface area (S), pore volume (V) and average pore diameter d_p (4V/S) of the investigated catalytic systems are listed in Table 1. For all the samples, the values of surface area and pore volume are lower than 10 m² g^{−1} and 0.04 cm³/g, respectively. The pore diameter is in the range 13–20 nm.

The X-ray diffraction patterns are shown in Fig. 1. All the samples present the characteristic peaks of a Ce_{0.75}Zr_{0.25}O₂ solid solution with a cubic fluorite structure of Fm3m symmetry, as expected for this Ce/Zr ratio [20,33]. In line with literature [20], for all the samples, an average crystallite size (D) near 15–20 nm was determined for the ceria/zirconia solid solution, by using the Scherrer equation:

$$D = \frac{K\lambda}{\beta \cos \theta}$$

where λ is the X-ray wavelength (1.541 Å), K the particle shape factor (taken as 0.9), β the width at half maximum and θ the diffraction angle of the considered peak.

No potassium crystalline phases were detected, thus suggesting that the deposited alkaline metal oxide phases are highly dispersed or mainly amorphous. Moreover the possible formation of K/Ce solid solutions cannot be completely ruled out even if the ionic substitution in the ceria lattice by potassium is unlikely due to the high dimension of potassium ion [34]. Diffraction peaks belonging to platinum and gold were also detected for CZKPt and CZKAu, respec-

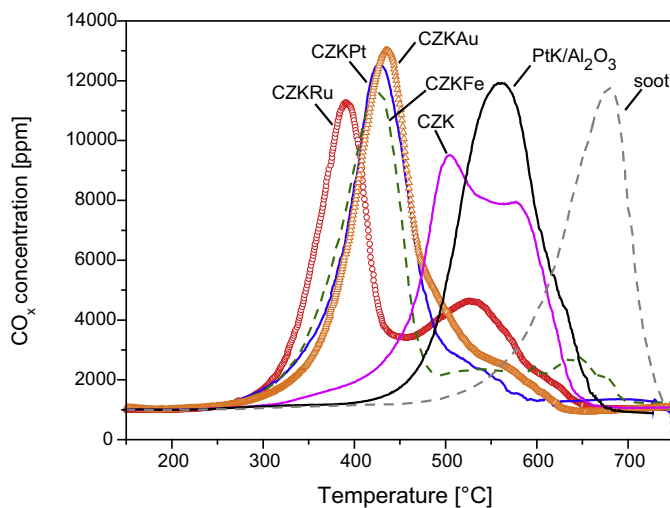


Fig. 2. Results of TPO experiments in $\text{He} + \text{O}_2$ (3% v/v) in presence of H_2O (1% v/v) + CO_2 (0.1% v/v).

tively. The average crystallite size, determined using the Scherrer equation, is 45 nm for both Pt and Au. SEM analyses were further performed over CZKPt and CZKAu samples which showed the presence of Pt and Au aggregates up to 200–300 nm.

The absence of peaks related to iron and ruthenium phases in the XRD profile of CZKFe and CZKRu may indicate the formation of Ce/Fe and Ce/Ru solid solutions, respectively [35–40]. Of note the possible incorporation of iron or ruthenium in the ceria fluorite lattice (i.e. the substitution of Ce ions with smaller Fe or Ru ions) could result in the contraction of the cell volume and explain the peak shifts, to higher 2θ angles, observed for both CZKFe and CZKRu samples [35,37,41,42]. This contraction was evident from the unit cell parameters obtained from Rietveld refinement: 5.355 Å for the CZK sample vs 5.324 Å and 5.288 Å for CZKFe and CZKRu, respectively, which confirm the possible incorporation of Fe and Ru in the fluorite lattice.

Finally, inductively coupled plasma (ICP) analysis was performed for the CZKRu sample which showed K and Ru contents near the theoretical loading in spite of the severe calcination conditions here adopted (i.e. final calcination in air at 900 °C for 10 h).

3.2. Soot oxidation activity in the presence of oxygen

The performances in the soot combustion of the Ceria/Zirconia-based catalysts were investigated by TPO experiments. The obtained results are shown in Fig. 2 in terms of CO_x ($\text{CO}_2 + \text{CO}$) evolution and compared with those obtained in the case of pure soot and $\text{Pt-K/Al}_2\text{O}_3$ catalyst. The O_2 consumption profiles (not shown) are always symmetrical to those of CO_x . In all cases, a high selectivity to CO_2 is observed except for the un-catalyzed soot oxidation in which a significant CO formation was found (resulting in a CO_2 selectivity near 60%).

The temperature onset T_{on} (the temperature at which the CO_x formation exceeds 300 ppm) for the un-catalyzed soot oxidation is close to 480 °C, whereas the peak maximum is observed at 680 °C. In the case of $\text{Pt-K/Al}_2\text{O}_3$ -soot system, the onset of soot oxidation is observed at 415 °C, i.e. 65 °C below that of the un-catalyzed soot. After ignition, soot combustion proceeds rapidly: the peak maximum is observed near 560 °C, i.e. about 120 °C below that of the un-catalyzed soot. CO_2 selectivity near 99% is measured in this case. According to several literature reports [43–47] the observed increase in soot oxidation activity over K-containing catalysts can be attributed to the formation of low melting point compounds which can improve the surface mobility of the active species thus

favoring the soot–catalyst contact, that has been claimed as a key factor in the oxidation of soot [48,49]. The role of platinum was ascribed to a synergistic effect occurring between K and Pt [46,50] in which platinum is claimed to enhance the mobility of active species formed over the alkaline component thus improving the soot oxidation activity.

Fig. 2 shows that in the presence of the Ceria/Zirconia-based catalysts the combustion of soot is significantly enhanced. In all cases both the ignition temperature and the peak temperature for soot oxidation considerably decrease as compared to the bare soot and to the $\text{Pt-K/Al}_2\text{O}_3$ system as well. In fact, even for the undoped CZK sample the onset temperature for soot oxidation is near 330 °C, i.e. about 150 °C below that of bare soot. CO_2 selectivity near 95% is measured in this case. The beneficial effect of ceria-based materials on soot combustion is well known in the literature [21,22,24], and is ascribed to the redox activity of ceria and in particular to its ability to deliver oxygen from the lattice to the gas phase and hence to the carbon surface. Moreover, it is well established that addition of zirconia to ceria improves soot combustion activity by increasing its oxygen storage capacity, redox properties and in particular the thermal stability [19,20,33,51,52]. A promoting effect of potassium is also expected, where the alkaline metal likely favors the chemisorption of molecular oxygen [53].

Over the metal-doped CZK samples (CZKMe samples with Me = Ru, Pt, Au, Fe) a further significant increase in the reactivity is observed with respect to pure CZK. In all cases the onset temperature is monitored at temperatures lower than 300 °C, i.e. ca. 200 °C below that of the un-catalyzed soot system. The performances of the various catalysts are compared in Table 2 in terms of T_{on} (ignition temperature, i.e. the temperature at which the CO_x concentration exceeds 300 ppm), T_{max} (the temperatures corresponding to the maximum in the TPO profile), T_{10} and T_{50} (i.e. the temperatures required to reach 10 and 50% soot conversion, respectively), CO_2 selectivity. Slightly better results, in terms of all the considered parameters, were obtained for the Ru-containing catalyst: in particular the ignition temperature is observed near 270 °C, i.e. about 210 °C below that of bare soot. This also leads to a decrease in the maximum peak temperature ($T_{\text{max}} = 391$ °C) and in the temperatures corresponding to 10 and 50% soot conversion (T_{10} and $T_{50} = 351$ °C and 409 °C, respectively). The presence of Ru also increases the CO_2 selectivity: a value higher than 99% was measured in this case, which is similar to that obtained over the $\text{Pt-K/Al}_2\text{O}_3$ system. Of note, a few CZKMe samples show high-temperature peaks (or shoulders) in the TPO profiles (e.g. CZKRu, CZKFe). These effects are likely ascribed to partial dishomogeneity in soot/catalyst contact.

The results observed over metal-doped CZ catalysts are in line with several literature reports which indicate that doping ceria with proper cations (i.e. Fe [33,36,38,54], Ru [40,55,56], Pt [57,58] and Au [59]) positively affects soot oxidation performances, likely enhancing the red-ox properties and the oxygen storage/release capacity (i.e. the oxygen species mobility) of the catalytic materials.

Finally, in the case of the CZKRu sample, preliminary tests were performed to check the stability of this sample. For this purpose the catalyst was subjected to a few repeated TPO soot oxidation cycles with $\text{He} + 3\% \text{O}_2$ up to 700 °C. The results (herein not reported for brevity) indicated a quite stable and reproducible behavior.

3.3. NO_x storage activity

The capability of the Ceria/Zirconia-based catalysts to adsorb NO_x was investigated at 350 °C. The results obtained in the case of a rectangular step feed of NO in the presence of oxygen (3% v/v), H_2O (1% v/v) and CO_2 (0.1% v/v) are shown in Fig. 3, whereas the amounts of stored NO_x and the NO_2/NO ratio measured at saturation are reported in Table 2. The outlet NO_x ($\text{NO} + \text{NO}_2$) concentration curves

Table 2

Soot oxidation activity data (T_{on} , T_{max} , T_{10} , T_{50} and CO_2 selectivity) obtained from TPO experiments in oxygen (O_2 3% v/v + He). Stored NO_x up to steady state and NO_2/NO molar ratio at NO shutoff upon NO_x adsorption at 350 °C (NO 1000 ppm, O_2 3% v/v, H_2O 1% v/v, CO_2 0.1% v/v + He).

Catalytic systems	T_{on} [°C]	T_{10} [°C]	T_{50} [°C]	T_{max} [°C]	CO_2 sel. [%]	Stored NO_x @ 350 °C [mol/g _{cat}]	NO_2/NO @ 350 °C
Pt-K/Al ₂ O ₃	415	497	558	562	99.9	5.53E-04	0.58
CZK	330	445	527	505	95.3	4.80E-05	0.016
CZKRu	270	351	409	391	99.8	7.75E-04	0.85
CZKPt	270	364	430	427	98.5	9.31E-05	0.048
CZKAu	285	375	437	435	93.9	5.15E-05	0.020
CZKFe	270	360	427	423	95.4	5.52E-05	0.013

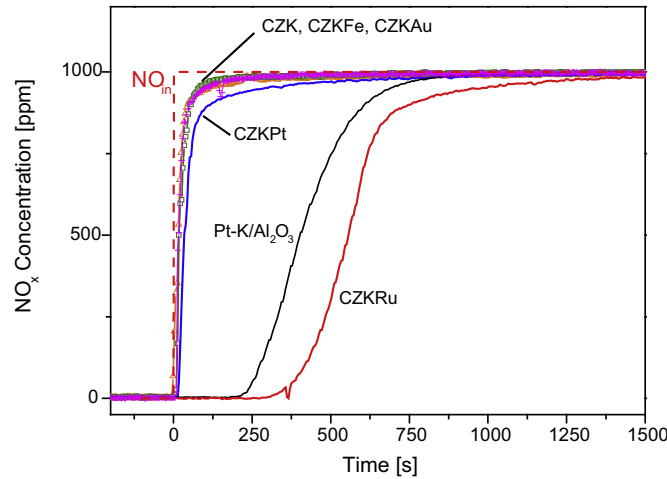


Fig. 3. Concentration profiles of NO_x during NO_x adsorption at 350 °C (1000 ppm NO and 3% O_2 in presence of H_2O (1% v/v) and CO_2 (0.1% v/v) + He).

are displayed as a function of time, along with that of the NO inlet concentration (dotted lines). For comparison purpose, the same experiments were also performed over the model Pt-K/Al₂O₃ sample.

In the case of CZKRu and Pt-K/Al₂O₃ samples, upon NO addition at $t = 0$ s, the NO_x outlet concentration presents a dead time indicating that NO_x fed to the reactor are entirely stored on the catalyst surface. Then the NO_x concentrations increase with time approaching the asymptotic concentrations corresponding to the NO inlet concentration (i.e. 1000 ppm), until catalyst saturation. Adsorbed NO_x of 7.75×10^{-4} and 5.53×10^{-4} mol NO_x/g_{cat} were estimated up to catalyst saturation over CZKRu and Pt-K/Al₂O₃ samples, respectively (Table 2). These amounts are in line with those reported in literature for very active LNT catalytic systems [29,30].

Of note, during the storage phase, both NO and NO_2 are detected at the reactor outlet (not shown in the figure), NO_2 formation being ascribed to the occurrence of the oxidation of NO by O_2 . In particular, the samples exhibiting the higher NO_x storage capacity also show the higher NO to NO_2 oxidation capability (NO_2/NO molar ratio of 0.85 and 0.58 for the CZKRu and Pt-K/Al₂O₃ samples, respectively).

A completely different picture is evident for all the other catalytic systems (i.e. CZK, CZKAu, CZKPt and CZKFe) which are not able to accomplish any relevant NO_x uptake. Indeed, upon the NO step addition no delay is observed in the NO_x outlet concentrations which closely resemble that of the inlet one. As a matter of fact, very low amounts of stored NO_x have been estimated (see Table 2). Moreover insignificant formation of NO_2 was observed in these cases (see the very low values of the NO_2/NO molar ratio, Table 2), pointing out a minor NO oxidation efficiency. In this respect, the high NO oxidation capability of the CZKRu sample is worth to note, much greater than the analogous Pt-containing sample (i.e. the CZKPt sample, $NO_2/NO = 0.048$). This might be related to the very

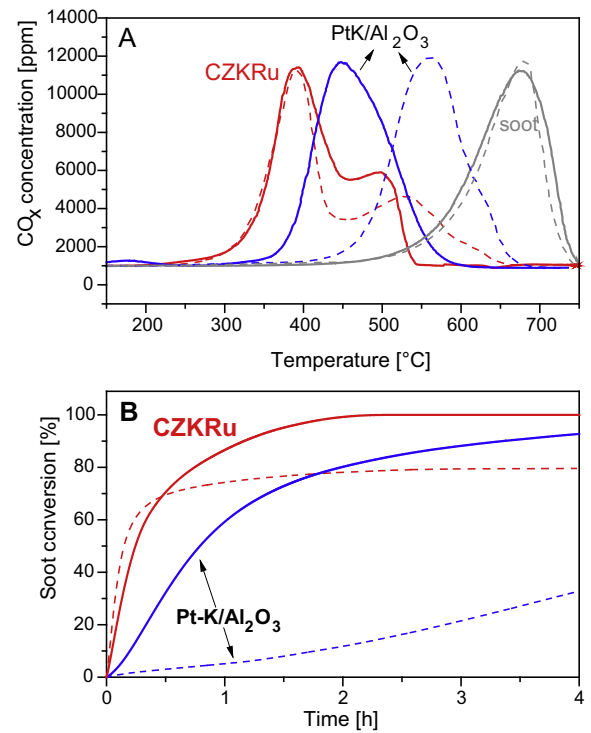


Fig. 4. Results of TPO experiments (A) and isothermal oxidation runs at 350 °C (B) performed over Pt-K/Al₂O₃ and CZKRu systems in 1000 ppm NO + 3% O_2 in presence of H_2O/CO_2 + He (solid lines) and in 3% O_2 in presence of H_2O/CO_2 + He (dashed lines).

different metal dispersion of the two samples, with Pt forming large clusters on the CZK surface (see above).

3.4. Soot oxidation activity of CZKRu in the presence of oxygen and NO

The soot oxidation activity was further investigated in the presence of oxygen and NO for the CZKRu catalyst, i.e. on the sample that showed the best catalytic performances in terms of soot oxidation and NO_x storage capacity. The Pt-K/Al₂O₃ sample was also considered for comparison purpose.

Fig. 4A shows the results obtained in the TPO experiments carried out with NO (1000 ppm)/ O_2 (3%, v/v) mixture in the presence of H_2O (1% v/v) + CO_2 (0.1% v/v) (solid lines). The results obtained in the case of the NO-free feed are also shown for comparison purpose (dashed lines).

As apparent from the figure, in the case of the uncatalyzed soot the presence of NO in the feed gas does not affect soot oxidation. Conversely, significant changes in the TPO profiles are observed in the case of Pt-K/Al₂O₃ catalyst, for which the beneficial effect of NO on soot combustion is evident. As a matter of fact a shift of ca. 110 °C towards lower temperatures is observed for the peak temperature. At variance, in the case of the CZKRu sample the peak temperature

is not greatly affected but soot oxidation is completed ca. 100 °C below that observed in the NO-free environment.

The effect of NO on soot oxidation was investigated under isothermal conditions as well (at 350 °C) and results are displayed in Fig. 4B in terms of soot conversion vs. time-on-stream in the presence of oxygen only (dashed lines) and of O₂/NO mixture (solid lines). In the presence of oxygen only the soot conversion over Pt-K/Al₂O₃ approaches 30% after 3 h. A much higher activity is apparent in the case of the CZKRu sample; in fact soot conversion approaches 80% after 1 h and then it keeps constant.

The presence of NO has a significant impact on soot oxidation, especially for the Pt-K/Al₂O₃ sample, where the soot conversion approaches 90% after 4 h (it was near 30% in the absence of NO). In the case of the CZKRu catalyst the effect of NO is less evident, in line with TPO experiments, and results in an increase of the amounts of soot combusted after 1 h. The positive effect of NO on soot combustion over Pt-containing catalysts is well known in the literature [60–63], and has been associated to the oxidation of NO into NO₂. The so-formed NO₂, which is a stronger oxidant than oxygen [25], promotes the low temperature soot oxidation according to the following overall reaction:



Notably, NO formed in reaction (1), can be re-oxidized into NO₂ (recycling of NO to NO₂) thus enhancing the efficiency of soot combustion. In addition to the above described NO recycle more recently it has been suggested that both Pt promotes soot oxidation also by a so-called cooperative reaction involving NO₂ and O₂, i.e. by enhancing O₂ chemisorption with the formation of oxygenated carbon complex which then react with NO₂, thus leading to an increased carbon combustion [64]. Finally, according to previous works [12,15], the possible participation of surface stored NO_x in soot combustion via a direct surface reaction cannot be excluded.

In the case of the CZKRu sample the effect of the presence of NO is less evident, due to the intrinsic high reactivity of the Me-doped CZK catalysts in soot combustion for the reasons discussed above. As a matter of facts, over the CZKRu sample, NO promotes soot oxidation at high temperatures (see TPO experiments) where the occurrence of the oxidation/recycling of NO to NO₂ is expected to favor soot combustion [22,58,65]. Moreover, the presence of ruthenium has been reported to increase the formation of surface oxygen complexes thus favoring the carbon-NO₂–O₂ oxidation [64,66,67].

3.5. Simultaneous removal of NO_x and soot

3.5.1. CZKRu and Pt-K/Al₂O₃ catalysts

The capability of CZKRu catalyst to accomplish the simultaneous removal of NO_x and soot was investigated alternating rectangular step feed of NO under lean condition (excess of oxygen) with rectangular step feed of H₂ under rich condition (absence of oxygen) separated by an He purge in between (ICSC experiments). For comparison purpose, the same experiments were performed over the model LNT Pt-K/Al₂O₃ system.

Preliminarily, *in situ* FTIR experiments were performed to gain information on the nature of the stored NO_x species, as detailed below.

3.5.1.1. Nature of stored NO_x species.

Fig. 5 shows the FT-IR spectra obtained upon admission of NO at 250 °C over Pt-K/Al₂O₃ (section A) and CZKRu (section B) at increasing contact times.

For both samples the formation of nitrites is observed. In particular, for Pt-K/Al₂O₃ catalyst (Fig. 5A), bands related to chelating nitrites at 1310 and 1237 cm⁻¹ ($\nu_{\text{sym.}}(\text{NO})$ and $\nu_{\text{asym.}}(\text{NO})$, respectively) and to linear nitrites at 1472 and 1075 cm⁻¹ ($\nu(\text{N=O})$ and $\nu(\text{N–O})$, respectively) are observed [68]. For CZKRu sample (Fig. 5B), $\nu_{\text{asym.}}(\text{NO})$ band related to chelating nitrites appears at 1244 cm⁻¹

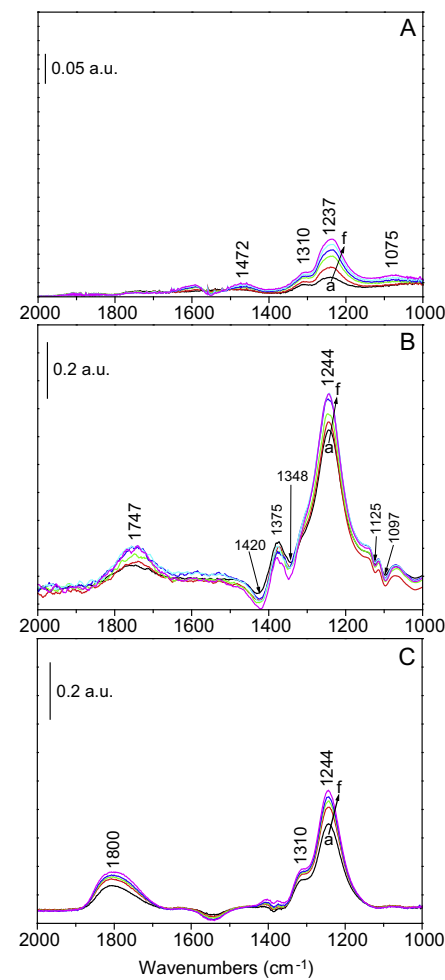


Fig. 5. FT-IR spectra of Pt-K/Al₂O₃ (A), CZKRu (B) and mechanical mixture (C) upon NO admission (5 mbar) after 30 s. (a), 1 min (b), 2 min (c), 3 min (d), 4 min (e) and 5 min (f) of contact.

and, upon increasing the exposure time, it increases in intensity faster than that of Pt-K/Al₂O₃ sample, reaching, after 5 min of contact, an intensity seven times higher than that observed for Pt-K/Al₂O₃. The presence of negative peaks at about 1420, 1348, 1125 and 1097 cm⁻¹ is related to carbonate species that are present on the surface and are eliminated by nitrite substitution. This makes the $\nu_{\text{sym.}}(\text{NO})$ band of chelating nitrites and any bands related to linear nitrites not evident, with the appearance of a false peak at 1375 cm⁻¹. Finally, CZKRu shows the presence of a broad band centered at about 1747 cm⁻¹ that is assigned to ruthenium mono-nitrosyls [65,69].

Fig. 6 shows the FT-IR spectra of Pt-K/Al₂O₃ (section A) and CZKRu (section B) obtained upon NO/O₂ admission at 250 °C at increasing contact times. As already reported in our previous works [30,68], at low exposure times mainly nitrites, of both chelating and linear type, are formed at the catalyst surface of Pt-K/Al₂O₃ (Fig. 6A), along with small amounts of ionic nitrates ($\nu_{\text{asym.}}(\text{NO}_3)$) and $\nu_{\text{sym.}}(\text{NO}_3)$ modes at 1385 and 1040 cm⁻¹, respectively) and bidentate nitrates ($\nu(\text{N=O})$ mode at 1513 cm⁻¹, $\nu_{\text{asym.}}(\text{NO}_2)$ and $\nu_{\text{sym.}}(\text{NO}_2)$ modes at 1317 and 1020–1000 cm⁻¹, respectively). Upon increasing the exposure time, the band at 1237 cm⁻¹ related to chelating nitrites increases and then, after 3 min of contact, decreases due to the nitrite oxidation into nitrates. Simultaneously, the bands characteristic of ionic and bidentate nitrates develop, so that after long exposure times (30 min) mainly nitrates are present at the catalyst surface. As discussed in a previous work [68] all the

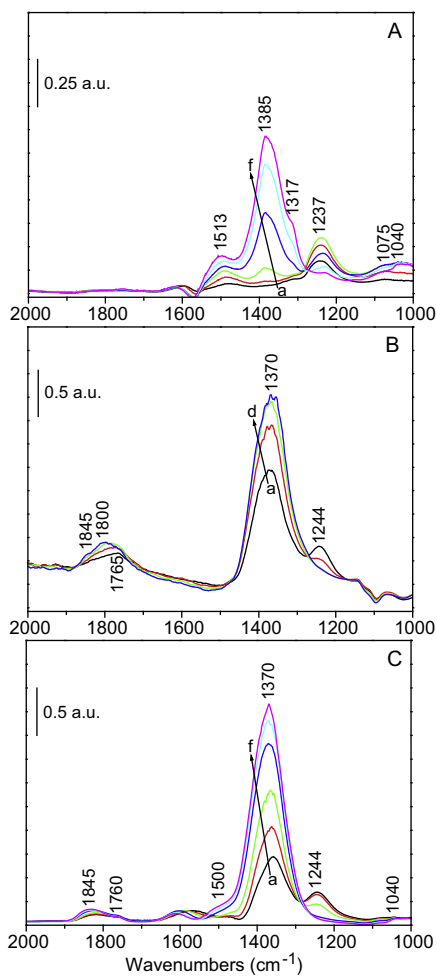


Fig. 6. FT-IR spectra of Pt-K/Al₂O₃ (A), CZKRu (B) and mechanical mixture (C) upon admission of NO/O₂ (1/4) mixture (pNO = 5 mbar) after 30 s. (a), 1 min (b), 3 min (c), 10 min (d), 20 min (e) and 30 min (f) of contact.

NO_x adsorbed species are related to the K phase which completely covers alumina.

Upon admission of the NO/O₂ mixture on CZKRu system (Fig. 6B), the initial formation of nitrites (1244 cm⁻¹) and nitrates (1370 cm⁻¹) is observed as well. However, in this case nitrites are quickly transformed into nitrates, being the maximum intensity of nitrite band reached after 30 s and completely eroded within 2 min, with the nitrate band predominant already after 30 s. Moreover, nitrate band becomes very intense and reaches saturation after only 3 min: the shape and the frequency of this band remember that of surface ionic nitrates on Pt-K/Al₂O₃ sample. However, taking into account the very low surface area of CZKRu sample and the higher amount of stored NO_x with respect to Pt-K/Al₂O₃ catalyst, as evidenced by catalytic tests (see below), it is reasonable that for CZKRu sample bulk nitrates are formed. This result is also confirmed by the absence of the band related to $\nu_{\text{sym}}(\text{NO}_3)$ mode that for completely symmetric bulk nitrates is IR silent. It is worth of note that this behavior is totally different with respect to that reported in literature for NO_x adsorption on Ce-Zr catalysts, pointing out the effect of Ru and K on Ce/Zr adsorption properties. In particular, Azambre et al. [70] studied NO/O₂ adsorption at 350 °C on a series of Ce_xZr_{1-x}O₂ mixed oxides by DRIFTS, showing the formation of a variety of bands related to surface bidentate nitrites and bidentate nitrates on all the samples. Very similar results were obtained by Haneda et al. [71] on Ce-Zr mixed oxides upon NO/O₂ admission at 200 °C.

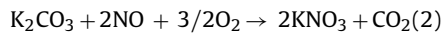
Finally, as in the case of pure NO, Ru mono-nitrosyl band is observed. However, differently from the case of pure NO, in the presence of NO/O₂ mixture more than one component is visible: at low contact times a band at 1765 cm⁻¹ is predominant, on increasing the contact time a component at 1845 cm⁻¹ becomes well visible and another one at 1800 cm⁻¹ becomes the more intense. On the basis of literature data [69], the component at 1765 cm⁻¹ can be ascribed to NO adsorbed on Ru⁰ and the components at higher wavenumbers can be assigned to partially oxidized Ru formed during the storage.

The results so far discussed point out, for the storage on CZKRu sample, the relevance of the “nitrite route” [29,72], which implies the stepwise oxidation of NO leading to the formation of nitrite adspecies as intermediate in the nitrate formation. At variance, in all cases the nitrate formation also proceeds through NO oxidation to NO₂, followed by NO₂ uptake as nitrate (“nitrate route”) via a disproportion reaction, in agreement with gas phase analysis showing the NO₂ formation (see below).

3.5.1.2. NO_x storage. The results obtained in the case of a rectangular step feed of NO (1000 ppm) in the presence of O₂ (3%, v/v), CO₂ (0.1%, v/v) and H₂O (1%, v/v) carried out at 300 °C on the Pt-K/Al₂O₃ catalyst in the absence and in the presence of soot are shown in Fig. 7A and B, respectively.

In the case of the soot-free system (Fig. 7A), upon NO step addition (at t = 0 s) the NO breakthrough is observed after ca. 200 s, which indicates an initial complete NO_x uptake. Also the evolution of NO₂, due to the occurrence of the oxidation of NO by O₂ over Pt sites, is seen starting from 250 s. Then the outlet concentrations of both NO and NO₂ increase with time and eventually reach a steady state level, indicating the saturation of the catalyst surface with NO_x. The amounts of NO_x stored at the end of the NO dose (steady-state) are near 6.2×10^{-4} mol/g_{cat}, as apparent from Fig. 8 (trace a, dotted line) which shows the amounts of NO_x stored as a function of time-on-stream.

Upon NO admission, CO₂ evolution is also observed. In fact the CO₂ concentration profile shows an initial peak from the background level of 1000 ppm. The increase in the CO₂ outlet concentration is due to the decomposition of surface carbonates upon NO_x uptake [7,10,12] in line with the stoichiometry of the following reaction:



At t = 2100 s the NO inlet concentration is switched off; after the switch a small tail is observed in the NO concentration profile, due to the desorption of weakly adsorbed NO_x species.

The results obtained in the case of the Pt-K/Al₂O₃ catalyst mixed with soot are shown in Fig. 7B. Also in the presence of soot, the NO_x outlet concentration shows a dead time and then increases approaching the asymptotic values corresponding to the NO inlet concentration. However in this case the NO_x breakthrough is lower than in the absence of soot (100 s vs. 200 s). Moreover, as apparent from Fig. 8 (trace A, solid line), the amounts of adsorbed NO_x at the end of the adsorption are near 5.5×10^{-4} mol/g_{cat}, i.e. a lower value if compared to that measured in the absence of soot (6.2×10^{-4} mol/g_{cat}). This indicates a negative effect of soot on the NO_x storage capacity which could be ascribed to the decrease of the NO₂ gas phase concentration [73,74,10–13]. In fact, K and soot are expected to compete for reaction with NO₂ leading to the observed decrease in the NO_x storage properties, being NO₂ involved in the soot combustion instead of nitrates formation. As a matter of fact, the NO₂ concentration at the reactor outlet in the presence of soot is significantly lower than that observed in the absence of soot (compare Fig. 7B and A) indicating the participation of NO₂ in the combustion of soot. As a result, in the presence of soot the NO₂/NO

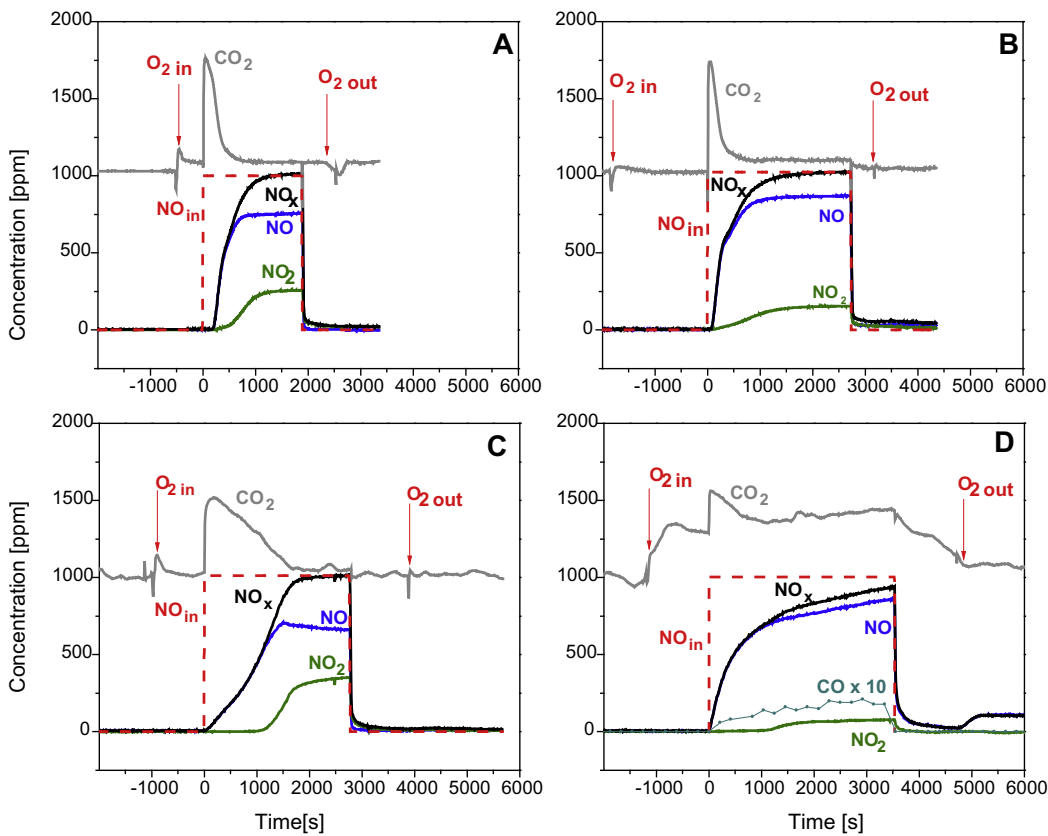


Fig. 7. Adsorption phase performed at 300 °C over Pt-K/Al₂O₃ (A and B) and CZKRU (C and D) in the absence (A and C) and presence (B and D) of soot with 1000 ppm NO and 3% O₂ in presence of H₂O (1% v/v) and CO₂ (0.1% v/v)+He.

molar ratio is lower than that measured in the case of the soot-free catalyst (0.18 vs. 0.34).

Also in the presence of soot, upon NO admission CO₂ evolution is observed, due to the decomposition of surface carbonates upon nitrates formation. However, at variance with the soot-free sample, after the initial peak the CO₂ concentration does not reach its background level but remains higher by 100 ppm indicating the occurrence of soot combustion. Notably, soot oxidation occurs only after NO addition to the reactor, since in the presence of oxygen alone no significant CO₂ formation is observed. Hence soot combustion can be ascribed mainly to NO₂ formed upon NO oxidation over Pt sites. Also, the participation of the stored NO_x in soot combustion via a direct surface reaction between the stored nitrates and soot cannot be excluded [12,15].

The same experiments were performed over CZKRU and CZKRU-soot mixture and the results are shown in Fig. 7C and D, respectively.

For the soot-free CZKRU system (Fig. 7C), upon NO admission to the reactor (at $t = 0$ s) NO is immediately observed at the reactor outlet whereas the NO₂ outlet concentration trace exhibits a dead time of ca. 1000 s. Notably, after breakthrough, the NO_x concentration increases very slowly with time indicating the large storage capacity of the CZKRU system. As a matter of fact, the overall amounts of NO_x that have been stored onto the catalyst surface are near 1.3×10^{-3} mol/g_{cat} (Fig. 8, trace b, dotted line), that is much higher with respect to the model Pt-K/Al₂O₃ catalyst (compare traces b and a). Moreover the NO₂ concentration measured at the reactor outlet at steady-state is higher than over the Pt/K sample (350 ppm vs. 250 ppm) pointing out the high NO to NO₂ oxidation capacity of CZKRU.

When the NO_x storage is carried out over the CZKRU-soot mixture (Fig. 7D), a slower NO_x uptake is observed with respect to the

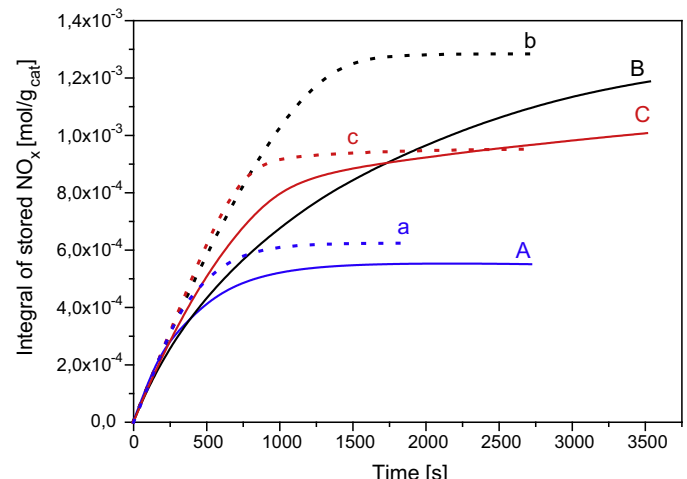


Fig. 8. Amounts of adsorbed NO_x versus time at 300 °C over Pt-K/Al₂O₃ (a and A), CZKRU (b and B) and Pt-K/Al₂O₃/CZKRU physical mixture (c and C) in the absence (dotted lines: a–c) and presence (solid lines: A–C) of soot.

pure CeZrKRU, as pointed out by the faster increase of the NO_x outlet concentration with time (compare Fig. 7D and C). Besides, also in this case the NO₂ concentration measured at steady state is lower than in the absence of soot due to the participation of NO₂ in the soot oxidation (see above). In spite of the slower rate of NO_x uptake, similar amounts of stored NO_x have been measured up to the end of the adsorption (1.2×10^{-3} mol/g_{cat} vs. 1.3×10^{-3} mol/g_{cat}), as pointed out by curves B and b of Fig. 8. Inspection of the same curves also shows that the presence of soot leads to an appreciable

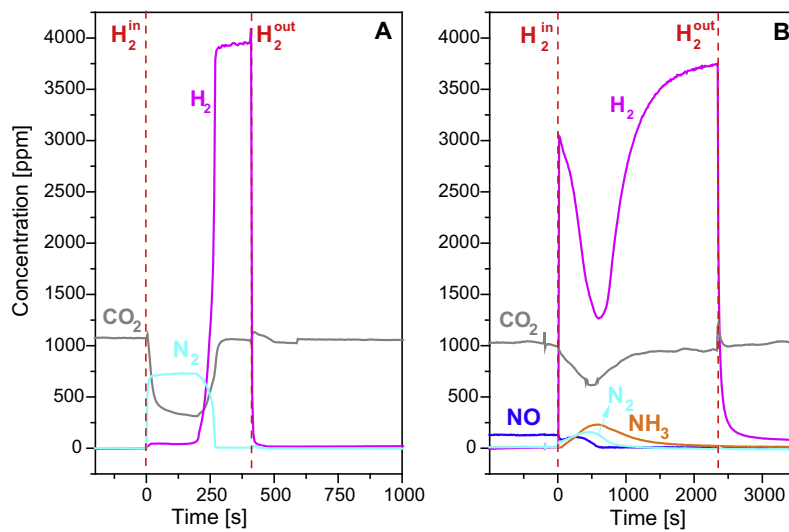


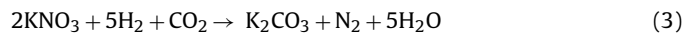
Fig. 9. Reduction phase performed at 300 °C over Pt-K/Al₂O₃ (A) and CZKRU (B) in the presence of soot with 4000 ppm H₂ in presence of H₂O (1% v/v) and CO₂ (0.1% v/v) + He.

decrease of the rate of NO_x adsorption, but it seems to affect in a lower extent the overall NO_x storage capacity of CZKRU.

Moreover, a significant production of CO₂ is detected at the reactor outlet in this case (see Fig. 7D), already upon O₂ addition. Then upon NO addition (at t = 0) the CO₂ production is further increased. Besides, the formation of low amounts of CO (i.e. ca. 20 ppm) is also observed. This confirms, in line with the TPO results, the higher soot combustion activity of CZKRU if compared to Pt-K/Al₂O₃.

3.5.1.3. NO_x reduction. After NO_x adsorption and helium purge, the reduction of the stored NO_x was carried out at the same temperature of adsorption (i.e. 300 °C) by admission of hydrogen. The results are shown in Fig. 9A and B for the Pt-K/Al₂O₃ and CZKRU catalysts, respectively. Only the data obtained in the presence of soot are shown.

In the case of the Pt-K/Al₂O₃-soot mixture (Fig. 9A), upon the addition of H₂ (at t = 0 s), the H₂ outlet concentration profile shows a dead time while N₂ is immediately produced. Then the N₂ concentration keeps constant for ca. 250 s and then decreases, in correspondence to H₂ breakthrough. Upon H₂ admission, a CO₂ uptake is also observed due to its re-adsorption onto the K sites once NO_x have been reduced, in line the stoichiometry of the overall following reaction:



The reaction is very fast and is limited by the concentration of H₂. Of note, the NO_x reduction is highly selective towards N₂ since no formation of byproducts like NO, ammonia or N₂O is observed. At the end of the reduction phase, the nitrates that have been stored during the previous lean phase have been fully removed from the catalytic surface, as confirmed by the N-balance performed at the end of the cycle (the amount of stored NO_x equal that of the N-containing species formed during the reduction phase).

A very different picture is evident in the case of the CZKRU-soot mixture (Fig. 9B). H₂ is only partially consumed and the evolution of N₂, NH₃ and NO is observed. H₂ is not immediately consumed upon admission to the reactor but an induction time is seen leading to the appearance of a minimum in the H₂ concentration, with a corresponding evolution of N₂ and NH₃.

These results indicate that over CZKRU sample the reduction of the stored NO_x is very slow if compared to the model Pt-K/Al₂O₃ catalyst. As a matter of fact the catalyst is not fully regenerated at the end of the reduction phase, as confirmed from the N-balance. Moreover the formation of NO and NH₃ leads to a poor N₂ selec-

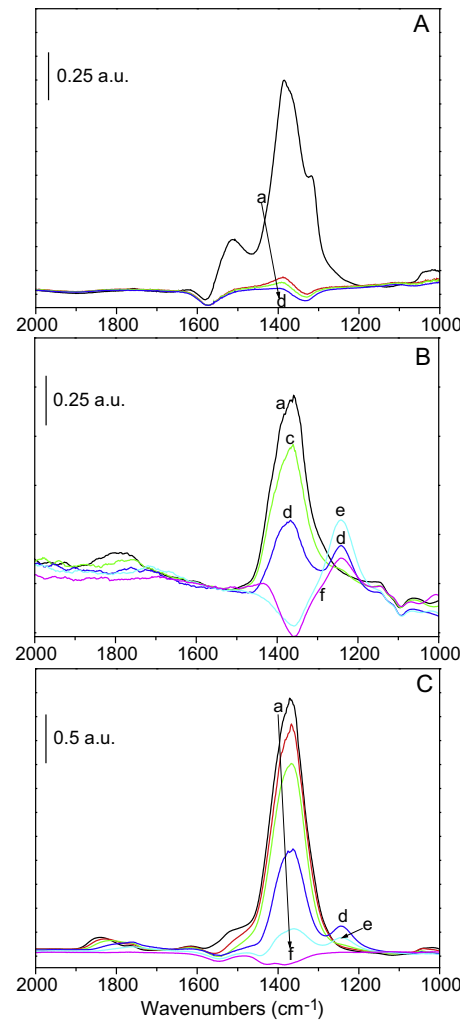


Fig. 10. Fig. 11 – FT-IR spectra of Pt-K/Al₂O₃ (A), CZKRU (B) and mechanical mixture (C) upon admission of H₂ (5 mbar) after (a) 30 s (b), 1 min (c), 5 min (d), 10 min (e) and 20 min (f). Spectrum a: after NO/O₂ storage and outgassing at 250 °C.

tivity, near 45%. Of note, in the case of CZKRU sample, as opposite to what observed in the case of Pt-K/Al₂O₃, the amount of H₂ consumed during the rich phase is higher than that expected on the

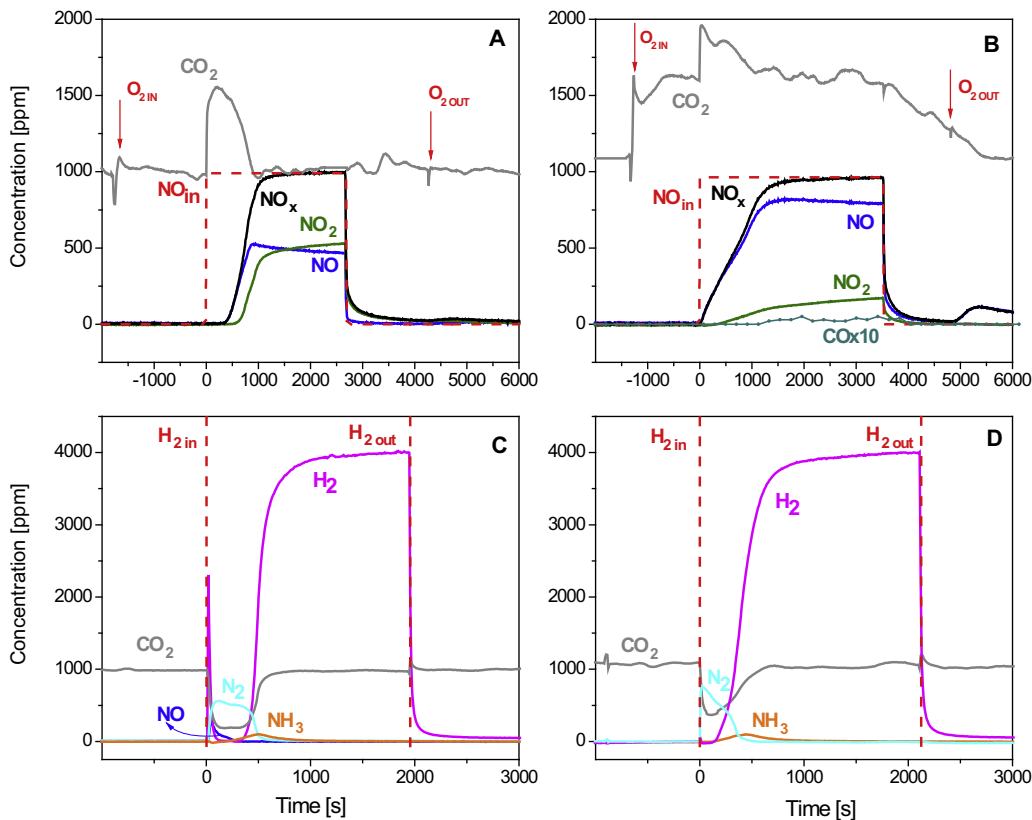


Fig. 11. Pt-K/Al₂O₃/CZKRU physical mixture: storage phase (T = 300 °C; 1000 ppm NO and 3% O₂ in presence of H₂O (1% v/v) and CO₂ (0.1% v/v)+He) in the absence (A) and presence (B) of soot; reduction phase (T = 300 °C; 4000 ppm H₂ in presence of H₂O (1% v/v) and CO₂ (0.1% v/v)+He) in the absence (C) and presence (D) of soot.

basis of formation of the reduction products. This overconsumption of hydrogen is due to the reduction of the CZ support.

The results obtained upon the reduction of the adsorbed NO_x species in the absence of soot (here not reported for brevity) are very similar to those obtained in the presence of soot indicating that the presence of soot does not significantly affect the reduction of the stored NO_x [10,12].

The reduction of stored nitrates was also studied by FTIR experiments by admitting hydrogen at 250 °C on the catalyst samples previously saturated with NO_x.

In the case of Pt-K/Al₂O₃ catalyst (Fig. 10A) the major part of surface nitrates is readily removed upon H₂ admission and the consumption of nitrates is almost completed already after 1 min, in agreement with catalytic tests. It is worth to note that no reduction intermediates are detected by FTIR spectroscopy.

On the contrary, in the case of the CZKRU sample (Fig. 10B) the reduction of stored nitrates proceeds slower upon H₂ admission and the formation of reduction intermediates such as nitrites (band at 1244 cm⁻¹) is observed. Of note, even after 20 min, the nitrites formed during the reduction are still present at the catalyst surface, in agreement with catalytic tests, which showed that the N mass balance does not close after a storage-reduction cycle (Fig. 9B). At the end of the reduction an intense negative peak at about 1360 cm⁻¹ related to bulk carbonates removed by nitrate storage is evident. Moreover, also the Ru carbonyl species are removed during the reduction.

3.5.2. Pt-K/Al₂O₃ – CZKRU physical mixture and double bed

The results reported so far pointed out that the CeZrKRU sample has a very high NO_x storage capacity and soot oxidation capability if compared to Pt-K/Al₂O₃ but is rather inefficient in the reduction of the stored NO_x. Based on these findings, to investigate possible

synergisms between the two catalyst samples, the reactivity of a physical mixture (loose contact) of the Pt-K/Al₂O₃ and CZKRU catalysts and of a double-bed of the same Pt-K/Al₂O₃ + CZKRU samples (separated by an inert layer in between) was further considered.

The results obtained over the Pt-K/Al₂O₃/CZKRU physical mixture during the NO_x adsorption in the absence of soot are shown in Fig. 11A. Upon NO addition (at t = 0 s) an initial complete uptake of NO is observed, which indicates the high storage capacity of this system. Then the NO_x concentration gradually increases with time approaching the asymptotic value corresponding to the NO inlet concentration, near catalyst saturation. The overall amount of NO_x that have been stored onto the catalyst surface is near 9.5×10^{-4} mol/g_{cat} (Fig. 8, trace c, dotted line) which is somehow intermediate between those of single Pt-K/Al₂O₃ and CZKRU samples (compare traces c, b and a of Fig. 8) and in line with the catalyst ratio of the physical mixture. Of note the physical mixture also shows a higher NO oxidizing capacity if compared to the single samples, as pointed out by the higher NO₂/NO ratio at steady state (i.e. 1.14 vs 0.53 and 0.34 for CZKRU and Pt-K/Al₂O₃, respectively).

FTIR experiments were performed also on the physical mixture to gain information on the nature of the stored NO_x species. Fig. 5C shows the FT-IR spectra obtained upon admission of NO at 250 °C at increasing contact times. Also in this case $\nu_{\text{asym.}}(\text{NO})$ band of chelating nitrites appears at 1244 cm⁻¹ that, as for CZKRU sample, increases faster than that of Pt-K/Al₂O₃, reaching a final intensity that is intermediate to those observed for the two pure samples. In this case, the corresponding $\nu_{\text{sym.}}(\text{NO})$ is well visible at 1310 cm⁻¹. Finally, the physical mixture, as the CZKRU sample, shows the presence of a broad band centered at about 1800 cm⁻¹ that is assigned to ruthenium mono-nitrosyls.

The FTIR spectra of the physical mixture recorded upon interaction with NO/O₂ (Fig. 6C) show features that are the sum of those

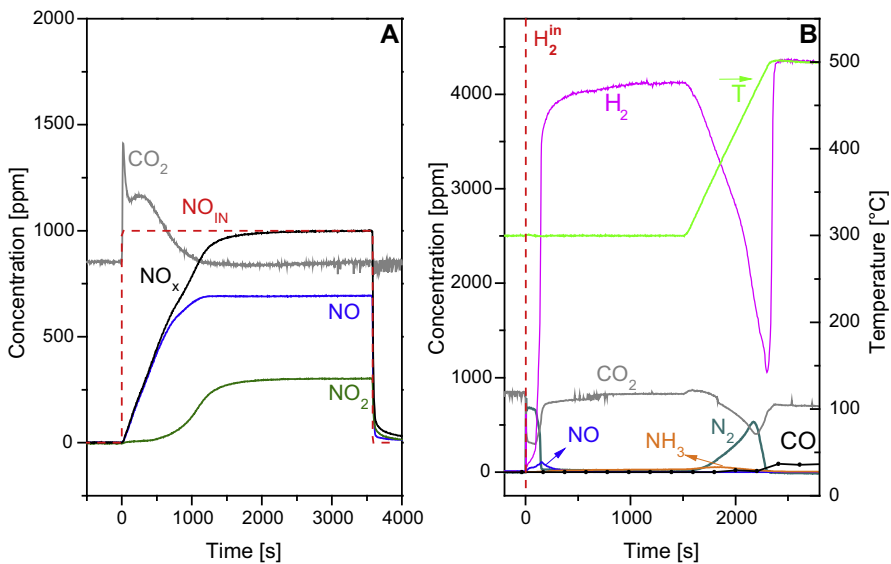


Fig. 12. Double-bed configuration (Pt-K/Al₂O₃/CZKRU): storage phase (T=300 °C; 1000 ppm NO and 3% O₂ in presence of H₂O (1% v/v) and CO₂ (0.1% v/v)+He) (A) and reduction phase (4000 ppm H₂ in presence of H₂O (1% v/v) and CO₂ (0.1% v/v)+He: isothermal reduction @ T=300 °C and subsequent temperature surface reaction from 300 °C to 500 °C) (B).

observed in the case of single Pt-K/Al₂O₃ and CZKRU samples. At low exposure times nitrites are formed which evolve to nitrates faster than in the case of Pt-K/Al₂O₃ catalyst, but slower than in the case of CZKRU sample. Accordingly only the bands of nitrates are present after 30 min, near catalyst saturation. As for the pure Ce/Zr sample the main contribution of bulk nitrates and formation of mono-nitrosyl species on Ru⁰ and Ru^{δ+} sites is apparent. Minor formation of nitrates on the K phase of the Pt-K/Al₂O₃ particles is also monitored by the weak bands at 1500 and 1040 cm⁻¹. In the range 1650–1550 cm⁻¹ a singular feature appears that is related to the overlap between combination of nitrate modes and the negative peak caused by the substitution of carbonates on Pt-K/Al₂O₃. As a matter of fact, the negative peak at about 1560 cm⁻¹ related to carbonates present on the surface and removed by nitrites/nitrates adsorption on Pt-K/Al₂O₃ catalyst is well visible also in Figs. 5 A, C and 6 A.

For comparison purpose the NO_x adsorption (in the absence of soot) was also carried out over the double-bed Pt-K/Al₂O₃ + CZKRU configuration and the results are shown in Fig. 12A. In this case, the overall amount of NO_x that have been stored onto the catalyst surface is near 8×10^{-4} mol/g_{cat}, very similar to that of the physical mixture. Moreover a NO_2/NO ratio near 0.43 was calculated at steady state which is somehow intermediate between those of single Pt-K/Al₂O₃ and CZKRU samples.

Finally, in the case of the physical mixture, the NO_x storage activity was further investigated in the presence of soot and results are shown in Fig. 11B. Upon NO addition (at t=0 s) no delay was observed in the evolution of NO_x which however increase very slowly with time. This points out the high storage capacity of this system, even in the presence of soot. As a matter of fact, 1.0×10^{-3} mol/g_{cat} of NO_x have been adsorbed up to catalyst saturation, (Fig. 8, trace C, solid line), indicating the negligible effect of soot on the overall NO_x storage capacity of the catalytic system (compare traces C and c).

In terms of soot oxidation activity, a very high CO_2 evolution is observed during the lean phase. In particular a synergistic effect is apparent in the case of the physical mixture with respect to the individual catalysts in that an higher production of CO_2 (near 600 ppm and 700 ppm before and after of NO admission, respectively) is observed, which outperforms that observed over both Pt-K/Al₂O₃ and CZKRU single samples. Moreover a negligible production of CO

is monitored (i.e. <5 ppm), resulting in a CO_2 selectivity higher than that of the single CZKRU single sample.

After NO_x adsorption and helium purge, the reduction of the stored NO_x was carried out at the same temperature of adsorption (300 °C). The results obtained over the physical mixture in the absence of soot are presented in Fig. 11C. Upon hydrogen addition (at t=0 s) a very sharp H_2 peak is observed and then H_2 is completely consumed. The immediate formation of N_2 is observed with very low amounts of NO and NH_3 . Indeed over the physical mixture the reduction is very fast, almost complete and also highly selective towards N_2 (i.e. N_2 selectivity near 84%), showing a behavior that is similar to that observed over Pt-K/Al₂O₃.

The reduction of stored nitrates over the physical mixture was also investigated by FTIR experiments by admitting hydrogen at 250 °C on the catalyst mixture previously saturated with NO_x (Fig. 10C). Like the pure CZKRU sample (Fig. 10B), the formation of nitrites is observed during the reduction. These nitrites are formed on the CZKRU particles as evidenced by the band position (1244 cm⁻¹) and by the fact that the formation of nitrites is not observed during the reduction with the single Pt-K/Al₂O₃ catalyst (Fig. 10A). The consumption of stored nitrates is faster than that observed over the single CZKRU sample and after 20 min no nitrites and nitrates remain on the surface, in agreement with catalytic tests. Also in this case Ru nitrosyls are reduced by hydrogen.

The results obtained over the double-bed Pt-K/Al₂O₃ + CZKRU catalysts are shown in Fig. 12B. The immediate formation of N_2 is observed, along with lower amounts of NO and NH_3 . However, as opposed to the physical mixture, the reduction of the stored NO_x is not complete under isothermal conditions. In fact more than 50% of the stored NO_x are reduced only upon heating the catalyst at higher temperatures (see Fig. 12B). This provokes the decomposition of the stored NO_x to NO and the subsequent reduction of the evolved NO over Ru sites. Notably, the production of small amounts of CO is also evident at high temperatures, due to the occurrence of the Reverse Water Gas Shift (RWGS) reaction:



The reduction of the stored NO_x over the physical mixture has also been carried in the presence of soot (Fig. 11D). Upon the addition of H_2 (at t=0 s), the H_2 outlet concentration profile shows a dead time during which it is completely consumed. The evolution

at first of N_2 and then of NH_3 is observed. No formation of other products (e.g. NO) was detected in appreciable amounts, resulting in a N_2 selectivity near 86%.

The reactivity of the physical mixture in the reduction of the stored NO_x is worth noticing, and points out a synergistic effect between the Pt-K/ Al_2O_3 and the CZKRu samples leading to the complete reduction of the stored NO_x . In fact both catalytic activity data and FTIR experiments prove that the NO_x species stored on both the Pt-K/ Al_2O_3 and the CZKRu samples are effectively reduced by H_2 , at variance with that observed in the case of the pure CZKRu catalyst and of the catalyst double bed where NO_x species remain adsorbed at the end of the reducing treatment. This points out that in the physical mixture the NO_x species stored on the CZKRu particles are reduced by H_2 thanks to the presence of the Pt-K/ Al_2O_3 sample.

In previous studies on the reactivity of Pt/ Al_2O_3 and Ba/ Al_2O_3 physical mixtures [75] we have shown that nitrates stored over Ba/ Al_2O_3 cannot be reduced in spite of the presence of Pt/ Al_2O_3 , at variance with that observed in the present study. According to Kumar et al., over Pt-Ba/ Al_2O_3 catalysts the NO_x reduction occurs via the transport of the stored NO_x from the BaO phase to the Pt/BaO interface, pointing out the occurrence of spillover processes from Ba sites to Pt involving the stored NO_x species [76]. Accordingly the data obtained over the Pt/ Al_2O_3 –Ba/ Al_2O_3 physical mixture indicate that the NO_x spillover process is not occurring among different catalyst granules. On these basis, NO_x spillover processes can be hardly invoked to explain the effective reduction of the NO_x stored over CZKRu in the Pt-K/ Al_2O_3 –CZKRu physical mixture. At variance, an inter-particle hydrogen spillover can be suggested, where H_2 activated over the Pt-K/ Al_2O_3 granules spills onto the CZKRu particles leading to the effective reduction of the Ru sites and hence of the stored NO_x species. In other words, it is suggested that the presence of Pt-K/ Al_2O_3 favors the reduction of the active Ru sites in CZKRu via inter-particles H_2 spillover phenomena. Along similar lines, Nabaho et al. have invoked inter-particle hydrogen spillover phenomena to explain the catalytic effect of Pt on the reduction of supported Co_3O_4 in a Pt/ Al_2O_3 + Co/ Al_2O_3 mixture [77]. In fact these authors demonstrated that Pt improves the reducibility of the Co_3O_4 phase despite the physical separation of Pt from Co. The results obtained in the case of the double-bed configuration, where Pt-K/ Al_2O_3 and CZKRu particles are separated by an inert layer, are in line with the occurrence of inter-particle hydrogen spillover phenomena when the Pt-K/ Al_2O_3 and CZKRu particles are in contact. In fact in the case of the double bed configuration H-adatoms formed onto the Pt-K/ Al_2O_3 particles cannot spill over CZKRu particles and this eventually prevents the full reduction of the stored NO_x at the adsorption temperature.

4. Conclusions

In this work we have investigated the catalytic behavior of ceria/zirconia (CZ) based catalysts, doped with Pt, Au, Ru or Fe and containing K, in both soot oxidation and removal of NO_x and the results were compared with that of a model Pt-K/ Al_2O_3 LNT catalyst.

It was found that all the CZ formulations promote soot oxidation in the presence of oxygen at temperatures below 300 °C. In particular the CZKRu sample showed a soot ignition temperature which is 150 °C below that of Pt-K/ Al_2O_3 .

Moreover, the analysis of NO_x storage activity carried out at 350 °C revealed that, among the investigated CZ systems, only the Ru-containing catalysts (CZKRu) is able to store NO_x showing a storage capacity even greater than that of the reference Pt-K/ Al_2O_3 LNT catalyst.

Basing on these findings, the capability of the CZKRu catalyst to accomplish the removal of NO_x in the absence and in the presence

of soot was further investigated. It was found that the Ru-based sample is by far more active than Pt-K/ Al_2O_3 in the both soot combustion and NO_x storage capacity. In particular soot has a negligible effect on the amounts of stored NO_x , while for model Pt-containing catalysts a detrimental effect of soot was observed.

In situ FTIR experiments were also performed to gain information on the nature of the stored NO_x species. On both CZKRu and Pt-K/ Al_2O_3 the initial formation of nitrites was observed which evolve fast to nitrates, particularly in the case of Ru-containing sample. Of note, for CZKRu the contribution of bulk nitrates, instead of only surface ionic nitrates for Pt-K/ Al_2O_3 , and formation of mono-nitrosyl species on Ru were observed, which is line with the high NO_x storage activity observed for the Ru-catalyst. However, the CZKRu sample showed a poor reactivity in the reduction of the stored NO_x by H_2 , possibly because the reductant is not readily activated by Ru. However a significant improvement of the NO_x reduction efficiency was attained when CZKRu is mixed with the Pt-K/ Al_2O_3 LNT sample (physical mixture). In line with literature proposals, it was suggested that in this case ruthenium is reduced by H-adatoms formed onto the Pt-K/ Al_2O_3 particles and spilled over the CZKRu particles.

In conclusion, the results point out that a physical mixture of Pt-K/ Al_2O_3 –CZKRu catalytic systems ensures high catalytic performances in both the deSoot and de NO_x activity. Bearing also in mind that ruthenium is much cheaper than platinum, this makes mixed LNT/CeZr catalytic systems potential candidates for the simultaneous removal of NO_x and soot from diesel exhausts.

Acknowledgement

LC acknowledges the financial support from MIUR (Futuro in ricerca, FIRB 2012, project SOLYST).

References

- [1] S. Brandenberger, O. Kröcher, A. Tissler, R. Althoff, *Catal. Rev. Sci. Eng.* 50 (2008) 492–531.
- [2] N. Takahashi, H. Shinjoh, T. Iijima, T. Suzuki, K. Yamazaki, K. Yokota, H. Suzuki, N. Miyoshi, S. Matsumoto, T. Tanizawa, T. Tanaka, S. Tateishi, K. Kasahara, *Catal. Today* 27 (1996) 63–69.
- [3] S. Matsumoto, *Catal. Today* 90 (2004) 183–190.
- [4] M.V. Twigg, *Catal. Today* 163 (2011) 33–41.
- [5] B.A.A.L. van Setten, M. Makkee, J.A. Moulijn, *Catal. Rev. Sci. Eng.* 43 (2001) 489–564.
- [6] K. Nakatani, S. Hirota, S. Takeshima, K. Itoh, T. Tanaka, SAE Paper SP-1674, 2002-01-0957, 2002.
- [7] L. Castoldi, R. Matarrese, L. Lietti, P. Forzatti, *Appl. Catal. B Environ.* 64 (2006) 25–34.
- [8] R. Matarrese, L. Castoldi, L. Lietti, P. Forzatti, *Top. Catal.* 42–43 (2007) 293–297.
- [9] R. Matarrese, L. Castoldi, L. Lietti, P. Forzatti, *Top. Catal.* 52 (2009) 2041–2046.
- [10] R. Matarrese, L. Castoldi, N. Artioli, E. Finocchio, G. Busca, L. Lietti, *Appl. Catal. B Environ.* 144 (2014) 783–791.
- [11] L. Castoldi, N. Artioli, R. Matarrese, L. Lietti, P. Forzatti, *Catal. Today* 157 (2010) 384–389.
- [12] N. Artioli, R. Matarrese, L. Castoldi, L. Lietti, P. Forzatti, *Catal. Today* 169 (2011) 36–44.
- [13] R. Matarrese, N. Artioli, L. Castoldi, L. Lietti, P. Forzatti, *Catal. Today* 184 (2012) 271–278.
- [14] R. Matarrese, L. Lietti, L. Castoldi, G. Busca, P. Forzatti, *Top. Catal.* 56 (2013) 477–482.
- [15] R. Matarrese, L. Castoldi, L. Lietti, *Catal. Today* 197 (2012) 228–235.
- [16] A. Trovarelli, C. de Leitenburg, M. Boaro, G. Dolcetti, *Catal. Today* 50 (1999) 353–367.
- [17] A. Setiabudi, J. Chen, G. Mul, M. Makkee, J.A. Moulijn, *Appl. Catal. B Environ.* 51 (2004) 9–19.
- [18] E. Aneggi, M. Boaro, C. de Leitenburg, G. Dolcetti, A. Trovarelli, *J. Alloy Compd.* 408–412 (2006) 1096–1102.
- [19] I. Atribak, F.E. López-Suárez, A. Bueno-López, A. García-García, *Catal. Today* 176 (2011) 404–408.
- [20] E. Aneggi, C. de Leitenburg, A. Trovarelli, *Catal. Today* 181 (2012) 108–115.
- [21] E. Aneggi, C. de Leitenburg, A. Trovarelli, *Catalysis by Ceria and Related Materials*, vol. 12, 2nd ed., Imperial College Press, 2013, pp. 565–621.
- [22] A. Bueno-López, *Appl. Catal. B: Environ.* 146 (2014) 1–11.
- [23] A.M. Hernández-Giménez, D. Lozano Castelló, A. Bueno-López, *Chem. Pap.* 68 (2014) 1154–1168.

[24] D. Fino, S. Bensaid, M. Piumetti, N. Russo, *Appl. Catal. A: Gen.* 509 (2016) 75–96.

[25] B.R. Stanmore, J.F. Brilhac, P. Gilot, *Carbon* 39 (2001) 2247–2268.

[26] P.L. Villa, Italian Patent Application No. MI2001A 001519 (17 July 2001).

[27] P.L. Villa, U.S. Patent 7,166,267, B2 (23 January 2007).

[28] K. Gallucci, P.L. Villa, G. Groppi, N. Usberti, G. Marra, *Catal. Today* 151 (197) (2012) 236–242.

[29] L. Castoldi, L. Lietti, I. Nova, R. Matarrese, P. Forzatti, F. Vindigni, S. Morandi, F. Prinetto, G. Ghiotti, *J. Chem. Eng. Chem. Eng.* J. 161 (2010) 416–423.

[30] L. Castoldi, L. Lietti, P. Forzatti, S. Morandi, G. Ghiotti, F. Vindigni, *J. Catal.* 276 (2010) 335–350.

[31] A. Setiabudi, M. Makkee, J.A. Moulijn, *Appl. Catal. B Environ.* 50 (2004) 185–194.

[32] I. Atribak, A. Bueno-López, A. García-García, *Combust. Flame* 157 (2010) 2086–2094.

[33] E. Aneggi, C. de Leitenburg, G. Dolcetti, A. Trovarelli, *Catal. Today* 114 (2006) 40–47.

[34] M.L. Ang, U. Oemar, Y. Kathiraser, E.T. Saw, C.H.K. Lew, Y. Du, A. Borgna, S. Kawi, *J. Catal.* 329 (2015) 130–143.

[35] G. Neri, A. Pistone, C. Milone, S. Galvagno, *Appl. Catal. B Environ.* 38 (2002) 321–329.

[36] Z. Zhang, D. Han, S. Wei, Y. Zhang, *J. Catal.* 276 (2010) 16–23.

[37] D. Jampaiah, K.M. Tur, S.J. Ippolito, Y.M. Sabri, J. Tardio, S.K. Bhargava, B.M. Reddy, *RSC Adv.* 3 (2013) 12963–12974.

[38] Z. Gu, X. Sang, H. Wang, K. Li, *J. Rare Earth* 32 (2014) 817–823.

[39] Q. Dai, S. Bai, Z. Wang, X. Wang, G. Lu, *Appl. Catal. B Environ.* 126 (2012) 64–75.

[40] M. Kurnatowska, W. Mista, P. Mazur, L. Kepinski, *Appl. Catal. B Environ.* 148–149 (2014) 123–135.

[41] H. Huang, Q. Dai, X. Wang, *Appl. Catal. B Environ.* 158–159 (2014) 96–105.

[42] F.J. Pérez-Alonso, M. López Granados, M. Ojeda, P. Terrores, S. Rojas, T. Herranz, J.L.G. Fierro, *Chem. Mater.* 17 (2005) 2329–2339.

[43] C.A. Querini, L.M. Cornaglia, M.A. Ulla, E.E. Miró, *Appl. Catal. B Environ.* 20 (1999) 165–177.

[44] A.L. Carrascull, M.I. Ponzi, E.N. Ponzi, *Ind. Eng. Chem. Res.* 42 (2003) 692–697.

[45] H. An, P.J. McGinn, *Appl. Catal. B Environ.* 62 (2006) 45–56.

[46] R. Matarrese, L. Castoldi, L. Lietti, P. Forzatti, *Catal. Today* 136 (2008) 11–17.

[47] L. Castoldi, R. Matarrese, L. Lietti, P. Forzatti, *Appl. Catal. B Environ.* 90 (2009) 278–285.

[48] J.P.A. Neeft, M. Makkee, J.A. Moulijn, *Chem. Eng. J.* 64 (1996) 295–302.

[49] J.P.A. Neeft, M. Makkee, J.A. Moulijn, *Appl. Catal. B Environ.* 8 (1996) 57–78.

[50] K. Krishna, M. Makkee, *Catal. Today* 114 (2006) 48–56.

[51] I. Atribak, A. Bueno-López, A. García-García, *Catal. Commun.* 9 (2008) 250–255.

[52] I. Atribak, A. Bueno-López, A. García-García, *J. Catal.* 259 (2008) 123–132.

[53] E. Aneggi, C. de Leitenburg, G. Dolcetti, A. Trovarelli, *Catal. Today* 136 (2008) 3–10.

[54] P. Venkataswamy, D. Jampaiah, K.N. Rao, B.M. Reddy, *Appl. Catal. A Gen.* 488 (2014) 1–10.

[55] D. Homsi, S. Aouad, J. El Nakat, B. El Khoury, P. Obeid, E. Abi-Aad, A. Aboukaïs, *Catal. Commun.* 12 (2011) 776–780.

[56] L.F. Nascimento, R.F. Martins, O.A. Serra, J. Rare Earth 32 (2014) 610–620.

[57] A. Bueno-López, K. Krishna, B. van der Linden, G. Mul, J.A. Moulijn, M. Makkee, *Catal. Today* 121 (2007) 237–245.

[58] B. Azambre, S. Collura, P. Darcy, J.M. Trichard, P. Da Costa, A. García-García, A. Bueno-López, *Fuel Process. Technol.* 92 (2011) 363–371.

[59] Y. Wei, J. Liu, Z. Zhao, A. Duan, G. Jiang, *J. Catal.* 287 (2012) 13–29.

[60] J. Oi-Uchisawa, A. Obuchi, Z. Zhao, S. Kushiyama, *Appl. Catal. B* 18 (1998) L183–L187.

[61] J. Oi-Uchisawa, A. Obuchi, A. Ogata, R. Enomoto, S. Kushiyama, *Appl. Catal. B Environ.* 21 (1999) 9–17.

[62] S.J. Jelles, R.R. Krul, M. Makee, J.A. Moulijn, *Catal. Today* 53 (1999) 623–630.

[63] S. Liu, A. Obuchi, J. Oi-Uchisawa, T. Nanba, S. Kushiyama, *Appl. Catal. B Environ.* 30 (2001) 259–265.

[64] M. Jeguirim, V. Tschamber, P. Ehrburger, *Appl. Catal. B Environ.* 76 (2007) 235–240.

[65] M. Guo, F. Ouyang, D. Pang, L. Qiu, *Catal. Commun.* 38 (2013) 40–44.

[66] V. Tschamber, M. Jeguirim, K. Villani, J. Martens, P. Ehrburger, *Appl. Catal. B Environ.* 72 (2007) 299–303.

[67] M. Jeguirim, K. Villani, J.F. Brilhac, J.A. Martens, *Appl. Catal. B Environ.* 96 (2010) 34–40.

[68] F. Prinetto, M. Manzoli, S. Morandi, F. Frola, G. Ghiotti, L. Castoldi, L. Lietti, P. Forzatti, *J. Phys. Chem. C* 114 (2010) 1127–1138.

[69] E. Guglielminotti, F. Bocuzzi, M. Manzoli, F. Pinna, M. Scarpa, *J. Catal.* 192 (2000) 149–157.

[70] B. Azambre, I. Atribak, A. Bueno-López, A. García-García, *J. Phys. Chem. C* 114 (2010) 13300–13312.

[71] M. Haneda, T. Morita, Y. Nagao, Y. Kintaichi, H. Hamada, *Phys. Chem. Chem. Phys.* 3 (2001) 4696–4700.

[72] L. Lietti, M. Daturi, V. Blasin-Aube, G. Ghiotti, F. Prinetto, P. Forzatti, *Chem. Catal. Chem.* 4 (2012) 55–58.

[73] J.A. Sullivan, O. Keane, A. Cassidy, *Appl. Catal. B Environ.* 75 (2007) 102–106.

[74] J.A. Sullivan, P. Dulgheru, *Appl. Catal. B Environ.* 99 (2010) 235–241.

[75] I. Nova, L. Lietti, L. Castoldi, E. Tronconi, P. Forzatti, *J. Catal.* 239 (2006) 244–254.

[76] A. Kumar, M.P. Harold, V. Balakotaiah, *J. Catal.* 270 (2010) 214–223.

[77] D. Nabaho, J.W. Niemantsverdriet, M. Claeys, E. van Steen, *Catal. Today* 261 (2016) 17–27.